J. Chem. Sci. (2020) 132:157
https://doi.org/10.1007/s12039-020-01859-1

REGULAR ARTICLE

Hydrogenation of furfural to furfuryl alcohol over efficient sol-gel nickel-copper/zirconia catalyst

MERVE ECE ŞEBIN, SOLMAZ AKMAZ* and SERKAN NACI KOC
Department of Chemical Engineering, Istanbul University-Cerrahpaşa, 34320 Istanbul, Turkey
E-mail: solmaz@istanbul.edu.tr

MS received 5 August 2020; revised 3 October 2020; accepted 13 October 2020

Abstract. Furfuryl alcohol (FA), a valuable compound from furfural (FF) was synthesized by efficient Ni-Cu/ZrO_2 catalysts. The catalysts with varying Ni and Cu loading were developed by sol-gel method and characterized by Brunauer-Emmet-Teller (BET) method, X-ray diffraction, Temperature Programmed Reduction (TPR), X-ray photoelectron spectroscopy techniques. Cu/ZrO_2 and Ni/ZrO_2 catalysts were also tested to compare the effect of the Ni-Cu/ZrO_2 catalyst. Both Ni and Cu showed the synergistic effect on FA formation. The Ni-Cu/ZrO_2 catalyst was used for hydrogenation of FF by changing pressure, catalyst loading, temperature and time. A 93% FA yield was achieved over the 7Ni-Cu/ZrO_2 catalyst with 0.07 g Ni and 0.1 g Cu/1 g ZrO_2 at 200 °C for 4 h under 1.5 MPa H_2 pressure. The sol-gel Ni-Cu/ZrO_2 catalyst without the use of expensive noble metals is effective on the hydrogenation of FF to FA relatively in mildly reaction pressure.

Keywords. Catalytic hydrogenation; furfural; furfuryl alcohol; sol-gel catalyst.

1. Introduction

Due to the concern of depletion of fossil fuels and environmental problems caused by fossil fuels in use, research on environmentally friendly renewable energy sources has increased. Biomass is an important resource in terms of being convertible into valuable substances for the energy and chemical industry. Furfural (FF) is one of the most used chemicals obtained from lignocellulosic biomass. FF has been known as an important platform material for the production of valuable chemicals in recent years.[1] 2-Methylfuran (MF) and furfuryl alcohol (FA) are among the most important valuable chemicals.[2] With the hydrogenation reactions of FF, 2-MF with the potential to be used as a fuel additive and FA with various application areas can be obtained. FA with a furan ring and hydroxymethyl group is obtained by hydrogenation of the C=O bond in the FF. FA is applied for the production of synthetic fibers and resins.[3] 2-Methylfuran is formed by the hydrogenolysis reaction of FA. 2-MF with a high octane number (103) has chemical and physical properties for use as a fuel additive (Scheme 1).[4]

The catalyst is one of the most important factors affecting product distribution in the hydrogenation reactions of FF. Studies are carried out on various hydrogenation catalysts. Noble metal-based catalysts generally used in hydrogenation reactions have also been tested for FF hydrogenation.[5,6] Studies on inexpensive catalysts for FF hydrogenation reactions have been focused on. Cu-based catalysts are among the commonly used catalysts for hydrogenation reactions, and the catalysts on different support materials such as Cu/SiO_2, Cu/TiO_2, Cu/TiO_2-SiO_2, Cu/MgO–Al_2O_3 and Cu/ZrO_2 catalysts were applied for the hydrogenation of FF.[7–10] Cu/TiO_2–SiO_2 catalyst provided 96.9% FF conversion and a 96.6% FA selectivity at gaseous phase[7] and an 89.3% FA selectivity at 100% FF conversion was obtained at 210 °C in isopropyl alcohol with Cu/MgO–Al_2O_3.[8] Besides single metallic catalysts, bimetallic catalysts are also frequently used for hydrogenation reactions. Fulajtarova *et al.*,[11] prepared Pd-Cu bimetallic catalyst by the impregnation method and a 98% FA selectivity was achieved at 110 °C under 0.6 MPa for 80 min. Srivastava *et al.*,[12] studied the hydrogenation reaction of FF to 2-MF with Cu-Co/Al_2O_3 catalyst and they obtained 2-MF with a maximum yield of 87% under 40 bar at 220 °C after 5 h. In the study of Fu *et al.*,[13] they prepared the Ni-Cu/Al_2O_3 catalyst by wet impregnation method and tested on the hydrogenation of FF. The activities of Ni and Cu on alumina support were also examined

*For correspondence

Published online: 21 November 2020

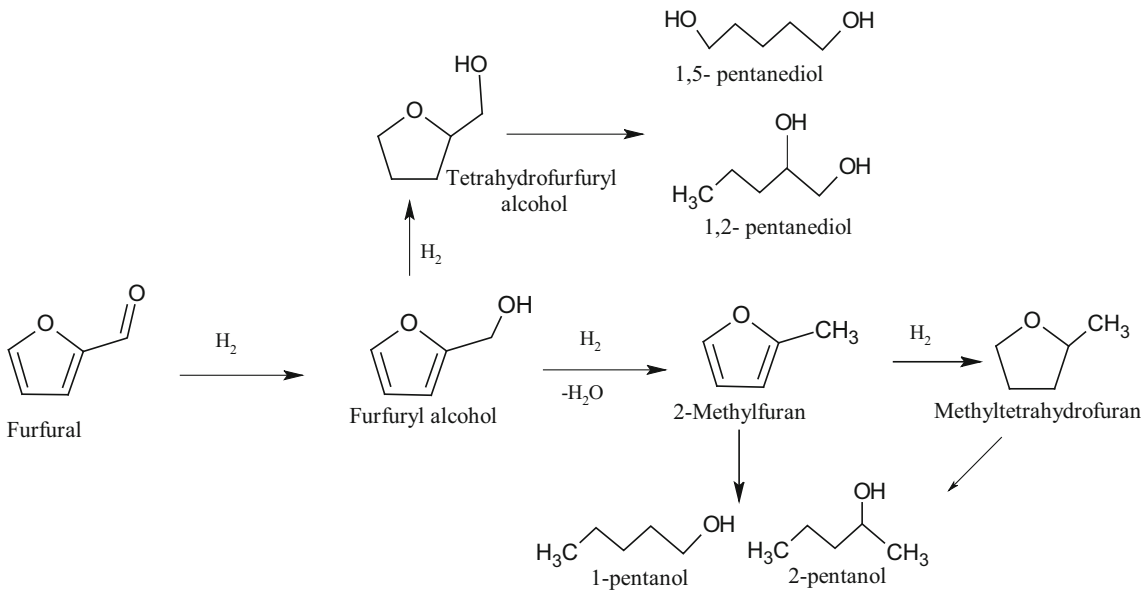

Scheme 1. Possible reaction pathway of furfural (FF) hydrogenation.[4]

separately, and it was stated that although Cu provided a low catalytic activity, with the addition of Ni, 100% conversion and a 92% 2-MF yield was achieved at 210 °C after 7 h with 10% Ni-10% Cu catalyst. Sulmonetti *et al.,*[14] worked on Ni-Mg-Al and Ni-Co-Al catalysts and the reactions were carried out in the continuous flow reactor at 155 °C, with a 5.5 mmol/h FF flow rate under a pressure of 1 atm. It was reported that the highest 71.8% FA selectivity with 98% FF conversion was obtained with 1.1Ni-0.8 Co/Al catalyst. Seemala *et al.,*[15] synthesized a 90% 2-MF yield in the presence of TiO_2 supported Ni-Cu catalyst at 200 °C for 8 h using 1,4-dioxane as a solvent under 3.5 MPa H_2 gas at 25 °C. The reduced sol-gel Ni-Cu catalyst on SiO_2 was used for FF hydrogenation by Khromova *et al.,*[16] and they reported 100% FA selectivity with approximately 80% FF conversion at 110 °C under 6 MPa pressure.

In studies, it is seen that Ni and Cu based catalysts are widely used.[13,15,17] Although the used metals are similar, very different reaction results can be obtained on different support materials. Moreover, as we searched, there are no studies on the effects of ZrO_2 supported Ni-Cu catalysts on FF hydrogenation. In our previous studies, Cu/ZrO_2 and $Co\text{-}Cu/ZrO_2$ sol-gel catalysts were developed and tested on FF hydrogenation. The Cu/ZrO_2 catalyst was effective on FA synthesis and 79.8% FA was obtained with this catalyst.[9] The $Co\text{-}Cu/ZrO_2$ catalyst provided a high yield of (94.1%) 2-MF.[10] This study aims to synthesize nickel-copper catalysts without expensive noble metals on ZrO_2 and to increase FA yield obtained by Cu/ZrO_2 catalyst. The sol-gel method, which is an effective method, was used for catalyst synthesis in order to ensure homogeneous metal distribution in the catalyst. Also, unlike other Ni-based studies, synthesized catalysts were used without reduction. The reactions were investigated under different reaction conditions in order to increase product yield and FF conversion. In order to increase the activity of the most effective catalyst, the effect of hydrogen pressure, catalyst loading amount, temperature and time on the reactions were also studied.

2. Materials and methods

2.1 *Materials*

Furfural (FF, ≥ 99%), isopropyl alcohol (IPA, HPLC grade), copper (II) nitrate trihydrate (>98%), nickel (II) acetate tetrahydrate (98%), zirconium propoxide (70%), 2-Methylfuran (2-MF, ≥99%) and furfuryl alcohol (FA, ≥99%) standards were provided from Sigma-Aldrich. Ethylacetoacetate (>98%, Merck) was purchased for catalyst preparation.

2.2 *Catalyst preparation*

Ni-based catalysts were prepared on ZrO_2 by the sol-gel method. For the preparation of Cu/ZrO_2, Ni/ZrO_2 and $Ni\text{-}Cu/ZrO_2$ catalysts, firstly 70% zirconium propoxide is dissolved in IPA and mixed in the polypropylene beaker for 30 min at room temperature. Ethyl acetoacetate, a ligand for gelation, is added and after that, nickel (II) acetate

tetrahydrate and/or copper (II) nitrate trihydrate in ultrapure water is also added to the mixture. The mixture is stirred at 60 °C. After gelation, it is dried at 80 °C overnight and calcined at 500 °C for 4 h.[9,10] The Ni-Cu/ZrO_2 catalysts containing Ni in amounts ranging from 0.05 g to 0.1 g were developed. The amount of copper was fixed at 0.1 g in the catalysts. The Ni-Cu/ZrO_2 catalysts containing Cu in amounts ranging from 0.05 g to 0.15 g at a fixed ratio of 0.07 g Ni/g ZrO_2 were also synthesized. The prepared catalysts were listed in Table 1.

2.3 *Catalyst characterization*

Surface area analysis of catalysts was applied by Brunauer-Emmett-Teller (BET) method and measured by Quantachrome Corporation, Autosorb-6 under nitrogen gas at 300 °C. X-ray diffraction (XRD) analyses were conducted with Rigaku D/Max-2200/PC XRD device with Cu–Kα irradiation (λ= 1.5404 Å). Surface compositions of catalysts were analyzed by Thermo Scientific K-Alpha X-ray photoelectron spectroscopy (XPS). The binding energies are referenced to the C1S line. Temperature programmed reduction (TPR) of catalysts was performed by HIDEN CATLAB^{TM} system with Hiden brand QIC-20 MS, mass spectrometer using 5% H_2/N_2 mixture at a rate of 5 °C/min. The elemental content of catalysts was detected with Thermo Elemental X Series 2 Inductive Coupling Plasma-Mass Spectrometry (ICP-MS).

2.4 *Catalytic reactions*

The reactions were carried out in Parr 4598 reactor system with a volume of 100 mL. 0.5 g of FF, 0.2 g of catalyst, 23 g of isopropyl alcohol (IPA) solvent, and 0.016 g of n-decane, an external standard for the product analysis, were used for each reaction. Purge was applied by 0.5 MPa hydrogen gas for 5 times to remove the air before the hydrogen gas was fed to the reactor. After the reactions were completed, the reactor was allowed to cool to room temperature. The catalyst was removed from products by filtration and products were analyzed by 7890A serial Agilent Technologies gas chromatography (GC) with a capillary column HP-5MS (30 m x 0.25 mm x 0.25 μm) and 5975C series mass spectroscopy (MS) system. Calibration curves were evaluated using FF, FA and 2-MF standards to determine product yields.[9,10]

Table 1. The labels and the contents of the catalysts.

Catalyst	Ni/g	Cu/g	ZrO_2/g
10Cu/ZrO_2	–	0.1	1
7Ni/ZrO_2	0.07	–	1
5Ni-Cu/ZrO_2	0.05	0.1	1
6Ni-Cu/ZrO_2	0.06	0.1	1
7Ni-Cu/ZrO_2	0.07	0.1	1
8Ni-Cu/ZrO_2	0.08	0.1	1
10Ni-Cu/ZrO_2	0.10	0.1	1
Ni-5Cu/ZrO_2	0.07	0.05	1
Ni-7.5Cu/ZrO_2	0.07	0.075	1
Ni-12.5Cu/ZrO_2	0.07	0.125	1
Ni-15Cu/ZrO_2	0.07	0.15	1

FF conversion, FA and 2-MF yields were calculated by using the following Equations (1), (2) and (3), respectively:

$$\text{FF conversion}\,(\%) = \frac{\text{consumed FF (mol)}}{\text{initial FF (mol)}} \times 100 \quad (1)$$

$$\text{FA yield}\,(\%) = \frac{\text{FA (mol)}}{\text{initial FF (mol)}} \times 100 \quad (2)$$

$$\text{2 - MF yield}\,(\%) = \frac{\text{2 - MF (mol)}}{\text{initial FF (mol)}} \times 100 \quad (3)$$

3. Results and Discussion

3.1 *Catalyst characterization*

The BET surface areas of catalysts are listed in Table 2. The surface area of the ZrO_2 sol-gel catalyst containing Ni is lower than that of the catalyst containing Cu. The surface area of ZrO_2 sol-gel catalyst containing Ni and 0.1 g Cu increases as the amount of Ni increases. In contrast, the surface area of the ZrO_2 sol-gel catalysts with 0.07 g Ni decrease as the amount of Cu increases from 0.05 g to 0.15 g. Moreover, the BET surface areas of fresh Ni-Cu/ZrO_2 catalyst and fifth used Ni-Cu/ZrO_2 catalyst are 45.1 and 14.5 $m^2\ g^{1-}$. The decrease in the surface area of the used catalyst is observed due to further crystallization by calcination.

The Cu, Ni and Zr amounts by weight (%) of the fresh and used 7Ni-Cu/ZrO_2 catalysts were measured by ICP-MS and listed in Table 3. It is observed that the amounts of Ni, Cu and Zr in the catalyst structure are almost preserved after the reaction.

X-ray diffraction (XRD) patterns of 7Ni/ZrO_2, 10Cu/ZrO_2, and 7Ni-Cu/ZrO_2 catalysts are shown in Figure 1.

The peaks at 2θ angles of 30.4°, 35.3°, 50.8°, 60.3°, and 74.9° represent tetragonal phase ZrO_2 (JCPDS card no: 701769) in the XRD pattern of Ni/ZrO_2. The same peaks were also observed in the XRD pattern of Cu/ZrO_2. However, the intensity of tetragonal ZrO_2 crystalline peaks decreased with both Ni and Cu loading. No CuO and NiO peaks were determined for all catalysts. It indicates that NiO and CuO were

Table 2. BET surface area of catalysts.

Catalyst	S_{BET} (m^2/g)	Catalyst	S_{BET} (m^2/g)
7Ni/ZrO_2	10.7	Ni-5Cu/ZrO_2	108.9
10Cu/ZrO_2	40.9	Ni-7.5Cu/ZrO_2	45.1
5Ni-Cu/ZrO_2	26.3	Ni-10Cu/ZrO_2	45.1
7Ni-Cu/ZrO_2	45.1	Ni-10Cu/ZrO_2 used	14.5
10Ni-Cu/ZrO_2	67.8	Ni-12.5Cu/ZrO_2	33.1
		Ni-15Cu/ZrO_2	15.2

Table 3. Metal amounts of fresh and used catalysts.

Catalyst	Cu (%)	Ni (%)	Zr (%)
Fresh 7Ni-Cu/ZrO_2	7.1	4.6	56.4
1st used 7Ni-Cu/ZrO_2	8.1	5.3	64.7
5th used 7Ni-Cu/ZrO_2	7.6	4.9	59.2

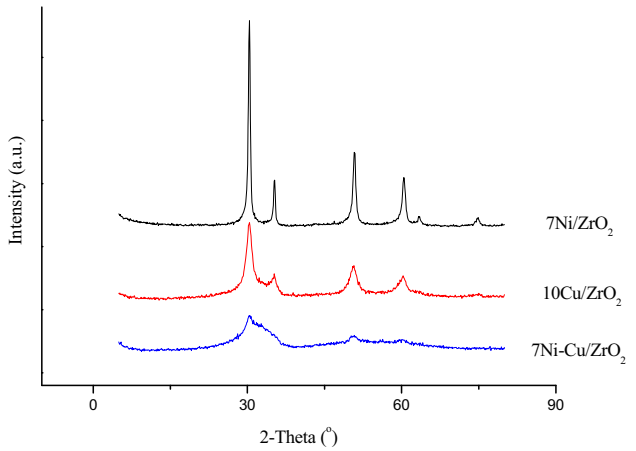

Figure 1. X-ray diffraction (XRD) patterns of 7Ni/ZrO_2, 10Cu/ZrO_2, and 7Ni-Cu/ZrO_2 catalysts.

uniformly dispersed on ZrO_2 due to the nature of sol-gel chemistry.

X-ray diffraction (XRD) patterns of Ni-Cu/ZrO_2 with 0.05 g, 0.06 g, 0.07 g Ni, 0.08 g and 0.1 g Ni and at a constant loading 0.1 g Cu are shown in Figure 2. The peaks of tetragonal ZrO_2 were also observed for all Ni-Cu/ZrO_2 catalysts. However, the intensities and the sharpness of ZrO_2 peaks, especially at 30.4 and 35.3°, decreased with the increase in the ratio of Ni incorporation up to 0.1 g.

X-ray diffraction (XRD) patterns of Ni-Cu/ZrO_2 with 0.05 g, 0.075 g, 0.1 g, 0.125 g and 0.15 g Cu at a constant loading of 0.07 g Ni are seen in Figure 3. The peak at 2θ = 30.4° shifted to higher 2θ angle value of 31.9° and 31.5° and the diffraction peak at 35.3° was

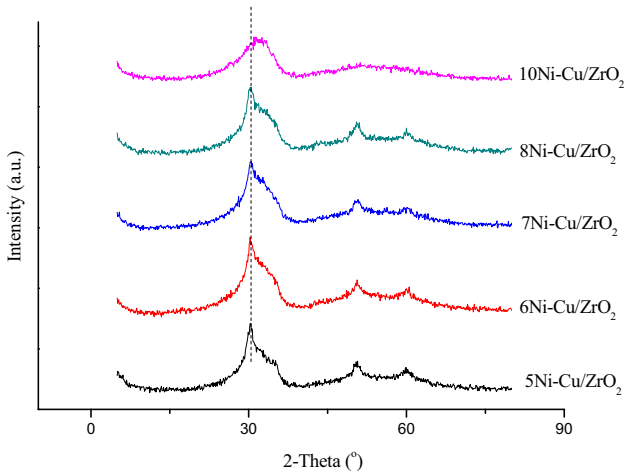

Figure 2. X-ray diffraction (XRD) patterns of Ni-Cu/ZrO_2 with 0.05 g, 0.06 g, 0.07 g, 0.08 and 0.1 g Ni and at a constant loading 0.1 g Cu.

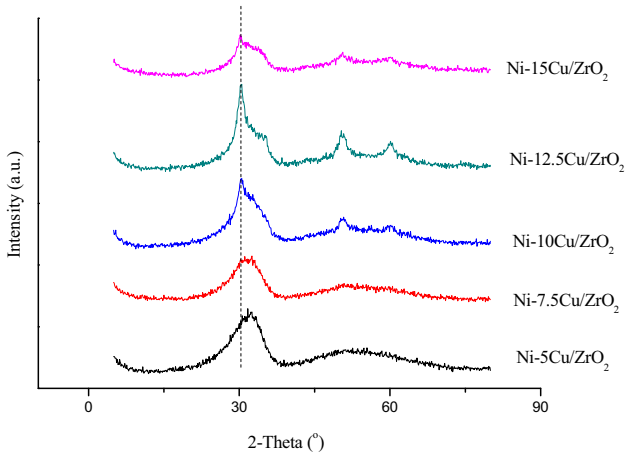

Figure 3. X-ray diffraction (XRD) patterns of Ni-Cu/ZrO_2 with 0.05 g, 0.075 g, 0.1 g, 0.125 g and 0.15 g Cu at a constant loading of 0.07 g Ni.

not observed in the catalysts with 0.05 g and 0.075 g Cu loading, respectively. Tetragonal peaks of the catalyst with 0.1 and 0.125 g Cu loading appeared and then slightly disappeared with 0.15 g loading at 50.8°, 60.3°, and 74.9°. This situation may be due to the Cu

incorporation to the zirconia matrix. It has been reported that the crystallinity of tetragonal ZrO_2 increases with increasing copper content then decreases again at 500 °C calcination temperature.[18] The peak at 35.3° can be also attributed to CuO (JCPDS card no: 050661) which may have appeared because of increasing of Cu loading.

As shown in Figure 4, there is no significant change in the X-ray diffraction (XRD) patterns of fresh, 1st used and 5th used 7Ni-Cu/ZrO_2 catalysts. However, a weak peak appeared at $2\theta = 43.1°$ which can be attributed to Cu^o (JCPDS card no: 04-0836), indicating that Cu^{2+} was reduced to Cu^o in the reducing reaction conditions.[9]

XPS measurements for Ni2p of 7Ni/ZrO_2 and 7Ni-Cu/ZrO_2 catalysts are shown in Figure 5a and b. The $Ni2p_{3/2}$ peaks at 855.1 eV and 857.2 eV can be attributed to Ni^{2+} (NiO) and multiplet-split Ni^{2+} (NiO), respectively.[19–24] Valente *et al.,*[20] assigned the binding energies peaks at 855.2 and 857.1 eV of NiO/ZrO_2 catalyst to Ni^{2+} and multiplet splitting. The Ni^{2+} peak (855.1 eV) represents the 3d↑hole. However, its mobility is strongly limited to be not 3d↓as a result of the repulsive Coulomb interaction between these holes. The multiplet splitting (857.2 eV) occurs due to electrons spin distribution of unpaired electron in the valence band. The multiplet splitting reveals the presence of various Ni^{2+} vacancies because of defect formation during calcination of the catalysts. In addition, two satellite peaks at 860.9 eV and 864.3 eV were observed, respectively. This indicates the two-d-hole bounding state, two 3d holes with↑and↓spins.[20,25–27] Furthermore, the XPS spectra of the 7Ni-Cu/ZrO_2 catalyst also showed the $Ni2p_{3/2}$ peaks at 854.8 eV and 856.5 eV in Figure 5b. The higher binding values of nickel species in the presence of only nickel indicating a stronger interaction of nickel species with ZrO_2.[28–30] The peaks of $Ni2p_{1/2}$ at 872.7 eV and 874.8 eV with two satellite peaks at 878.5 and 881.1 eV, which showed about 17.5 eV spin-orbit splitting (ΔE), were also observed for Ni^{2+} and Ni^{2+} (multiplet-split peak).[19,26,31] The higher $Ni2p_{3/2}$ peaks at 856.2 eV and 860.6 eV were also observed in the XPS spectra of the 1st used 7Ni-Cu/ZrO_2 catalyst in Figure 5c and no peak of metallic Ni was detected, indicating that no reduction occurred during the reaction.

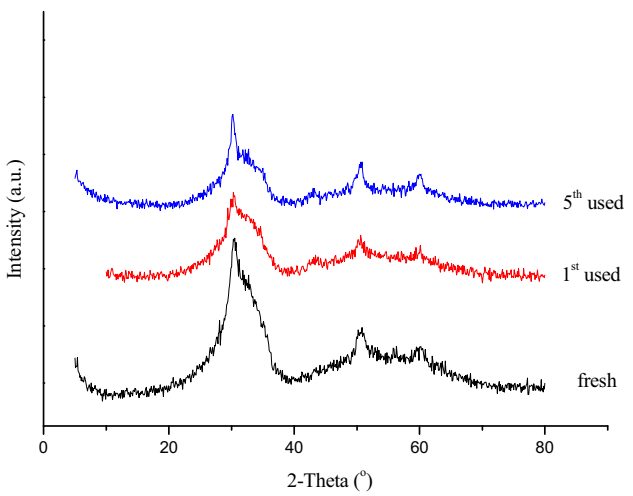

Figure 4. XRD patterns of fresh, 1st used and the 5th used Ni-Cu/ZrO_2 catalysts.

XPS measurements for Ni2p of 8Ni-Cu/ZrO_2 and 10Ni-Cu/ZrO_2 catalysts are shown in Figure 6a and b. Ni^{2+} peaks at 854 eV and 854.6 eV and multiplet-split Ni^{2+} peaks at 856.7 eV and 856.2 eV were also observed for 8Ni-Cu/ZrO_2 and 10Ni-Cu/ZrO_2 catalysts, respectively.

An XPS spectrum for Cu2p of 10Cu/ZrO_2 catalyst is shown in Figure 7a. The $Cu2p_{3/2}$ binding energy at 932.4 eV can correspond to Cu^+ and the binding energy at 933.8 eV can be assigned to Cu^{2+}.[32–34] Two satellite peaks at 941.1 eV and 943.5 eV proved the CuO. The $Cu2p_{1/2}$ binding energy at 953.4 eV with satellite peak at 962.0 eV indicates spin-orbit splitting (ΔE) of about 19.6 eV between $Cu2p_{3/2}$ and $Cu2p_{1/2}$ supporting the presence of Cu^{2+}.[34,35] Same peaks for Cu2p of 7Ni-Cu/ZrO_2 catalyst are also determined in the XPS spectra in Figure 7b. In addition, a peak at 935.6 eV in Cu/ZrO_2 catalyst and a peak at 934.6 eV in Ni-Cu/ZrO_2 were observed. As it has been reported in our previous studies,[9,10] this higher binding energy peak may be assigned to $Cu(OH)_2$[36,37] or strong interacting Cu^{2+}-O-Zr species because of the homogeneous structure of sol-gel chemistry.

As shown in Figure 7c and d, the peak at 933.7 eV disappeared at the first used and the fifth used catalysts, indicating that CuO species are reduced to Cu^0/Cu^+ under hydrogenation reaction. In addition, the peaks at 932 eV and 932.8 eV were observed at the first used and fifth used catalysts, respectively. Due to the difficulty of distinguishing the Cu^+ and Cu^0 peaks, 932 eV and 932.8 eV can be assigned to Cu^+ or Cu^0.[9,10,38–40] However, the peaks at 936.5 eV and 935.3 eV which may represent the strong interacting Cu^{2+}-O-Zr species, were not reduced.

XPS measurements for Cu2p of 8Ni-Cu/ZrO_2 and 10Ni-Cu/ZrO_2 catalysts are shown in Figure 8a and b. Cu^{2+} peaks at 932.9 eV and 933.2 eV were detected for 8Ni-Cu/ZrO_2 and 10Ni-Cu/ZrO_2 catalysts, respectively. The peak at 935.6 eV was observed at 8Ni-Cu/ZrO_2 catalyst. However, this peak was not

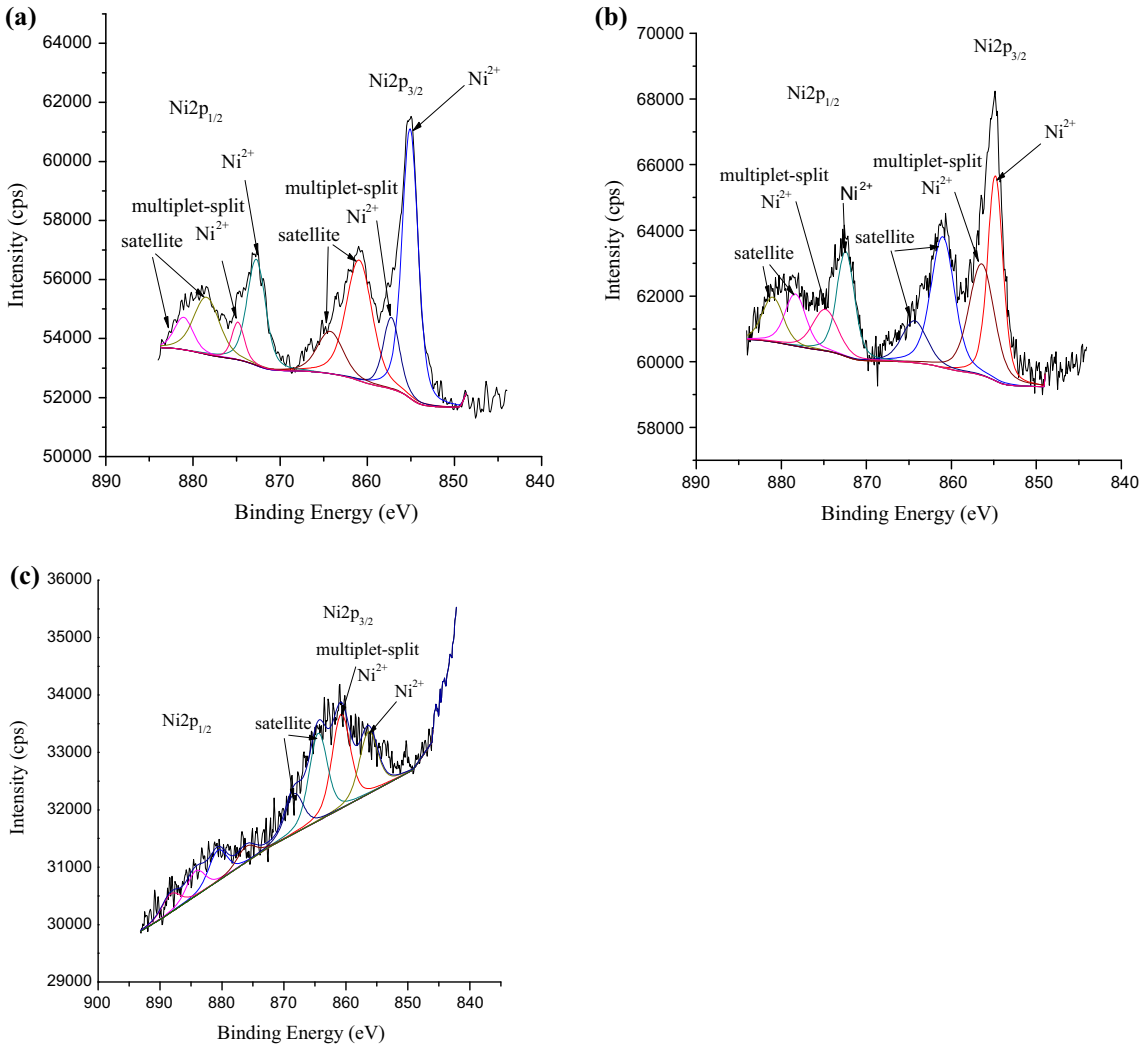

Figure 5. (**a**) Ni 2p XPS result of 7Ni/ZrO_2 catalyst (**b**) Ni 2p XPS result of fresh 7Ni-Cu/ZrO_2 catalyst (**c**) Ni 2p XPS result of 1st used 7Ni-Cu/ZrO_2 catalyst.

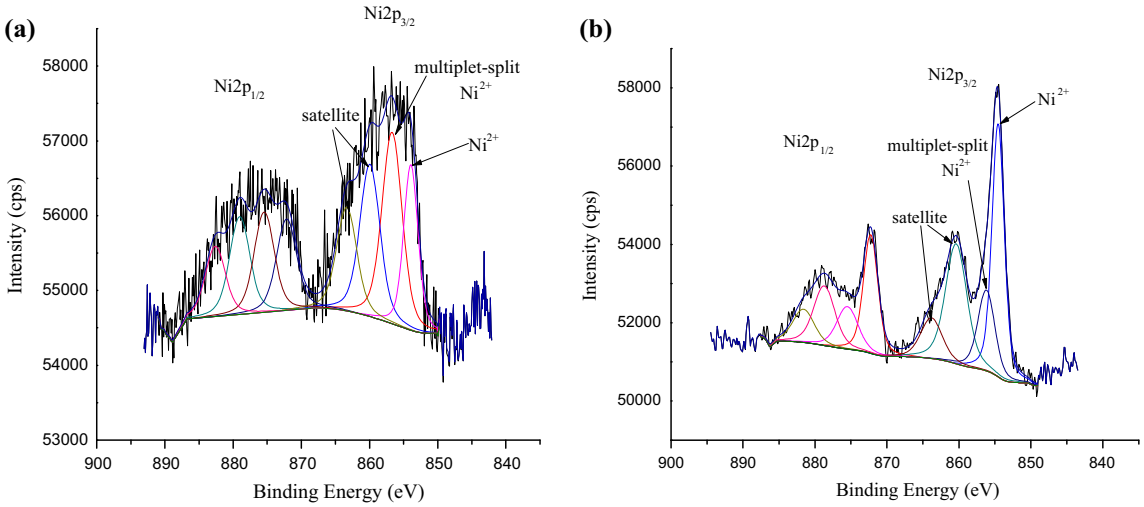

Figure 6. (**a**) Ni 2p XPS result of 8Ni-Cu/ZrO_2 catalyst (**b**) Ni 2p XPS result of 10Ni-Cu/ZrO_2 catalyst.

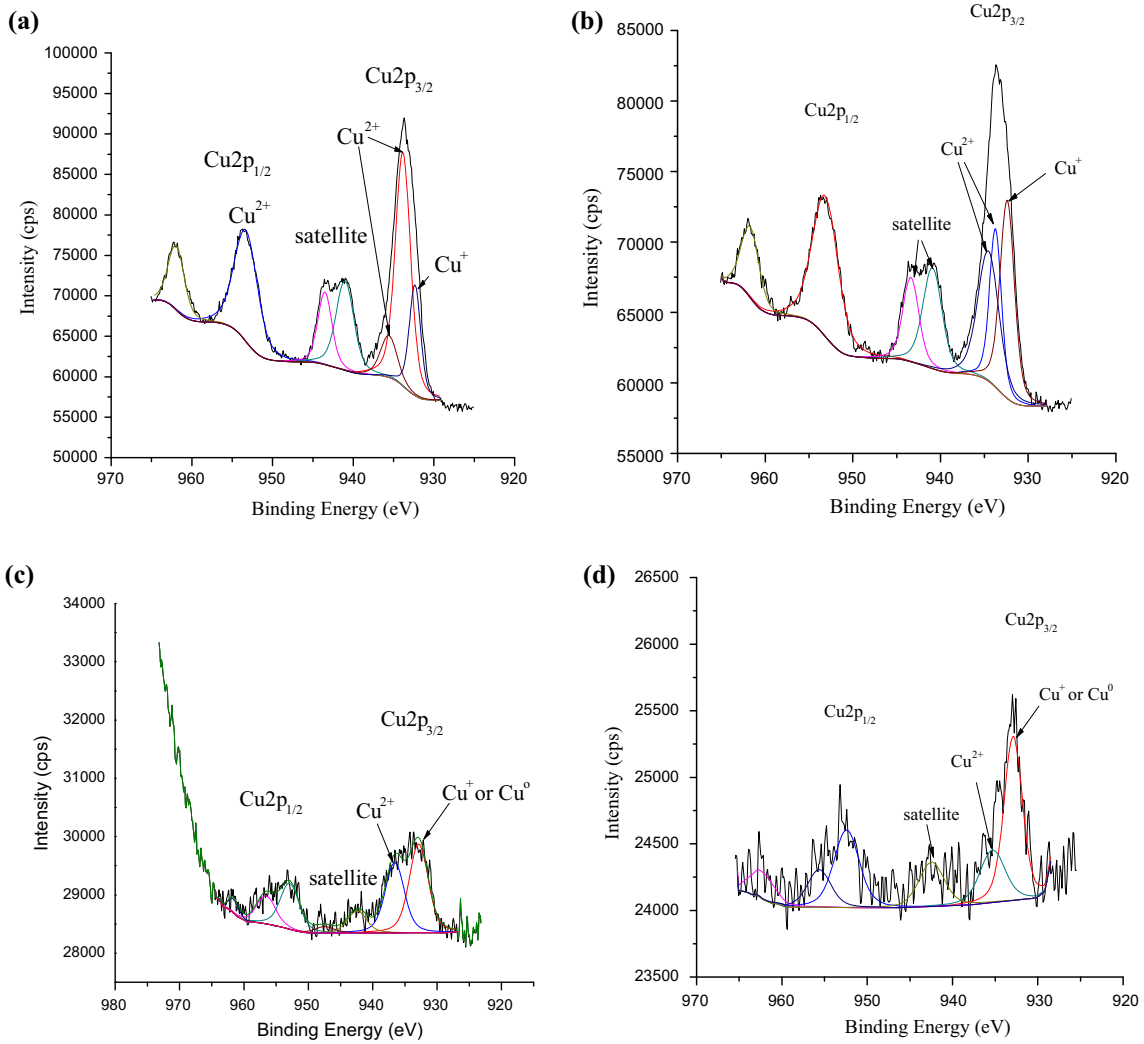

Figure 7. (**a**) Cu 2p XPS result of 10Cu/ZrO_2 catalyst (**b**) Cu 2p XPS result of fresh 7Ni-Cu/ZrO_2 catalyst (**c**) Cu 2p XPS result of the 1st used 7Ni-Cu/ZrO_2 catalyst (**d**) Cu 2p XPS result of the 5th used 7Ni-Cu/ZrO_2 catalyst.

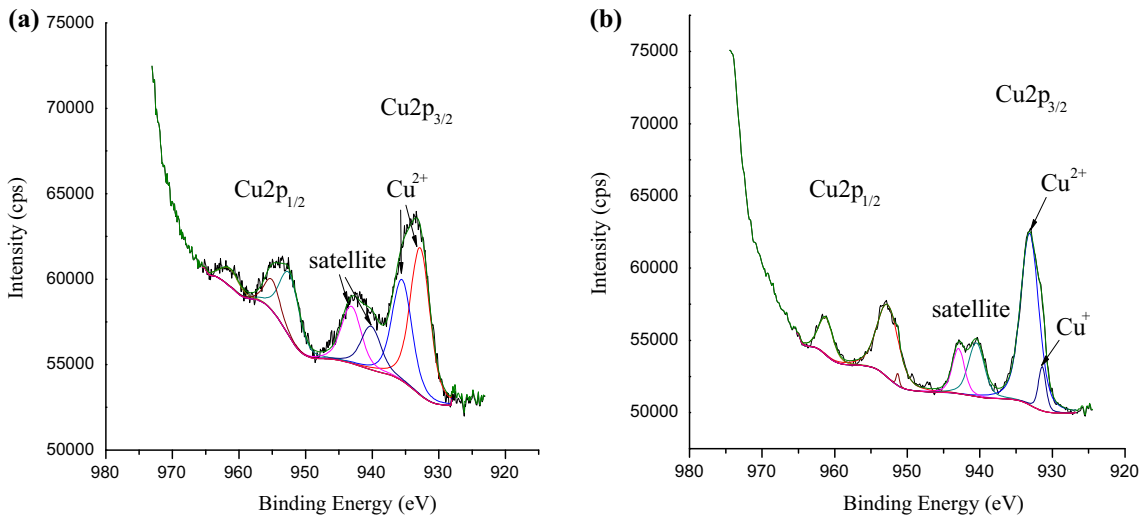

Figure 8. (**a**) Cu 2p XPS result of 8Ni-Cu/ZrO_2 catalyst (**b**) Cu 2p XPS result of 10Ni-Cu/ZrO_2 catalyst.

determined and the peak at 931.4 eV which can be attributed to Cu^{+} appeared in 10Ni-Cu/ZrO_2 catalyst.

The surface ratio of the Cu/Ni in the catalyst structure decreased from 1.09 to 0.91 with the increasing of Ni amount from 0.07 g to 0.1 g in the catalyst.

XPS spectra for Zr3d of 7Ni/ZrO_2, 10Cu/ZrO_2, 7Ni-Cu/ZrO_2 and the fifth used Ni-Cu/ZrO_2 catalysts in Figure 9a–d show characteristic $3d_{5/2}$ peaks at 181.7 eV, 181.7 eV, 181.5 eV, 181.9 eV and $3d_{3/2}$ peaks at 184.1 eV, 184.0 eV, 183.9 eV and 184.3 eV, respectively. The spin–orbit splitting of about 2.5 eV between the $3d_{5/2}$ and $3d_{3/2}$ peaks confirms the presence of Zr^{4+}.[20,41]

TPR measurements of the Cu/ZrO_2, Ni/ZrO_2, and Ni-Cu/ZrO_2 catalysts are shown in Figure 10. The Cu/ZrO_2 catalyst gave a reduction peak at 180.4 °C which can represent the reduction of copper oxide to metallic copper.[10,33] The peak starting at around 578 °C, which reveals the interacting Cu-O-Zr species, was also observed in our previous study.[10] The strong peak in the range of 400-700 °C can be attributed to the reduction of Ni^{2+} to Ni^{o}. The strong shoulder can be due to the strong Ni-ZrO_2 interaction. The Ni-Cu/ZrO_2 catalyst gave two reduction peaks at 200 °C which can be attributed to the reduction of copper oxide to metallic copper and at around 500 °C which can represent the reduction of nickel oxide to metallic nickel, respectively. Khromova *et al.,*[16] also determined the same two peaks at their Ni-Cu/SiO_2 sol-gel catalyst and they also explained that the broad peak of Ni reduction represents the strong interaction of nickel with SiO_2. The reduction of nickel oxide occurred at a lower temperature for the Ni-Cu/ZrO_2 catalyst, indicating hydrogen spillover effect along with reduction.[10]

3.2 *Catalytic hydrogenation reactions*

3.2a *The effect of Ni and Cu amount on Ni-Cu-ZrO_2 catalyst activity*: The effect of the amount of Ni and

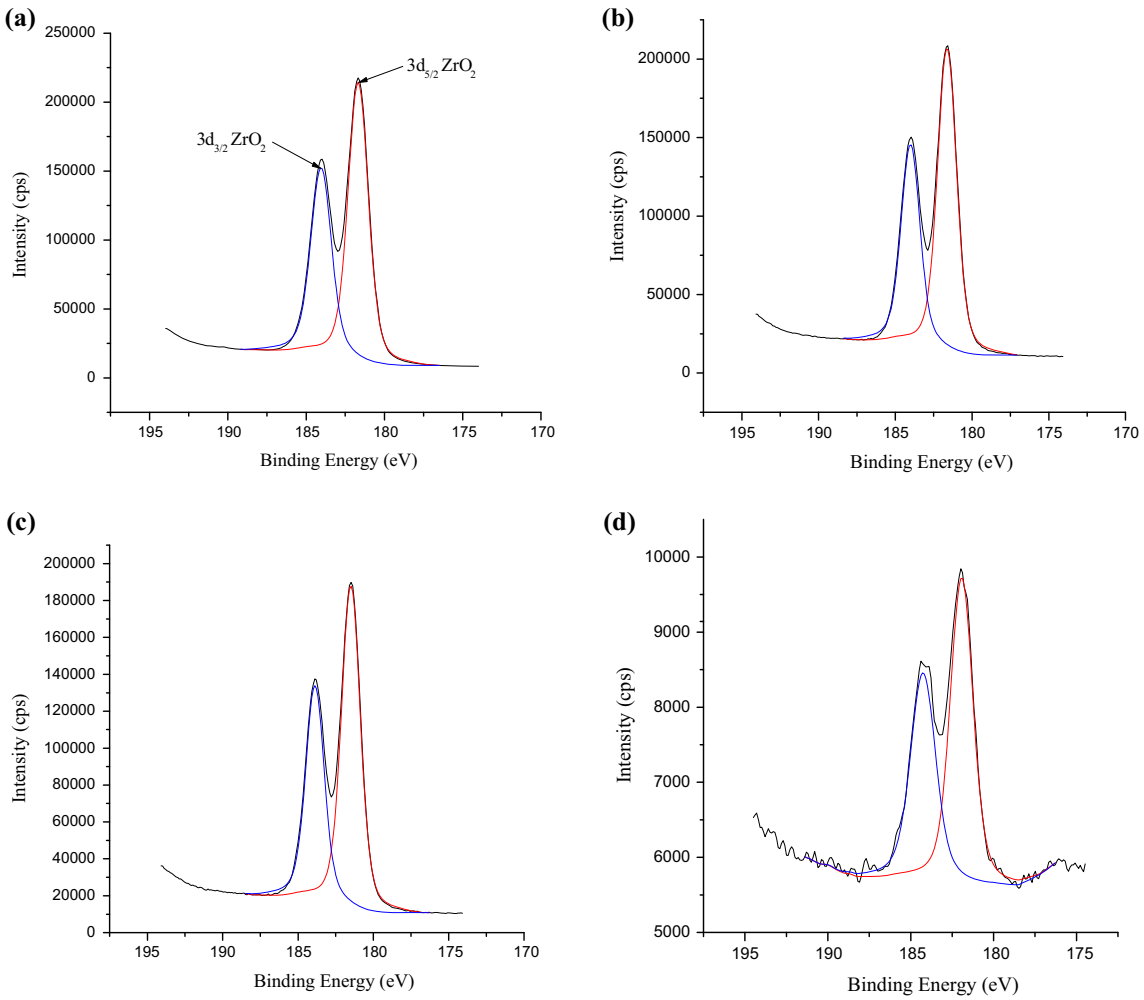

Figure 9. (**a**) Zr3d XPS result of 7Ni/ZrO_2 catalyst (**b**) Zr3d XPS result of 10Cu/ZrO_2 catalyst (**c**) Zr3d XPS result of fresh 7Ni-Cu/ZrO_2 catalyst (**d**) Zr3d XPS result of the fifth used 7Ni-Cu/ZrO_2 catalyst.

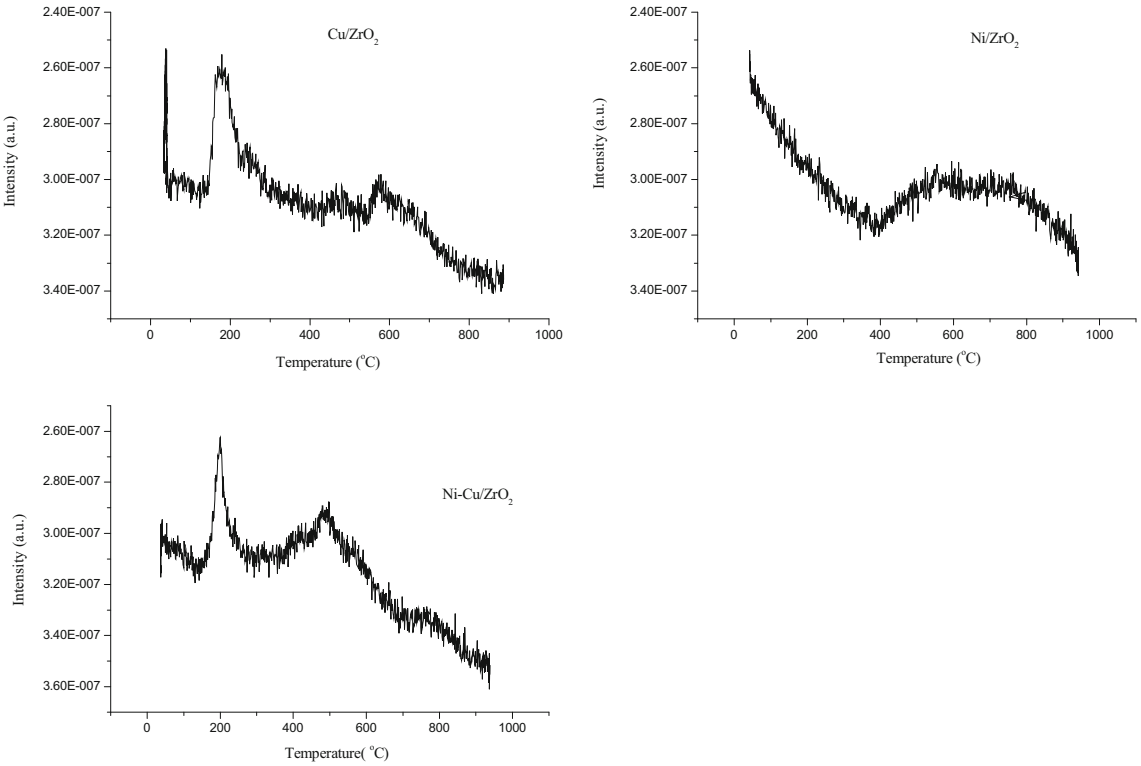

Figure 10. TPR measurements of the Cu/ZrO_2, Ni/ZrO_2, and $Ni\text{-}Cu/ZrO_2$ catalysts.

Cu on the $Ni\text{-}Cu/ZrO_2$ catalyst activity was investigated for the hydrogenation of FF. Firstly, $Ni\text{-}Cu/ZrO_2$ catalysts containing Ni in amounts ranging from 0.05 g to 0.1 g at a fixed ratio of 0.1 g Cu were developed using the sol-gel method. The catalytic reactions were carried out at 200 °C for 4 h under 1.5 MPa H_2 pressure at ambient temperature, and FA, 2-MF yields and FF conversions are given in Table 4. The by-product named "other" was not exactly determined by GC-MS which gave some possible predictions such as: 2-penthyl furan, furfuryl alcohol acetate, furan propanoic acid. "Other" may be due to the reaction of FF or reaction products with IPA.[10] With the increase in the amount of Ni from 0.05 g to 0.07 g in the $Ni\text{-}Cu/ZrO_2$ catalyst, the efficiency of the catalyst increased and FA yield reached 93.0% with 99.5% FF conversion. In addition, the by-product (other) decreased with the increase of Ni amount in the catalyst. The maximum 2-MF yield of 6.9% was obtained with the catalyst containing 0.06 g Ni and then decreased to 1.3% in the presence of the catalyst with 0.08 g Ni. As can be seen in Table 4, Ni mainly has an impact on the formation of FA and converts FF to FA. However, FA yield and FF conversion fell for further Ni ratio in the catalyst. FA and 2-MF yields decreased to 37.2% and 2.4%, respectively, with

Table 4. The effect of Ni amount in $Ni\text{-}Cu/ZrO_2$ catalyst with 0.1 g Cu on FA, MF yields and FF conversion.

Catalyst					
	$5NiCu/ZrO_2$	$6NiCu/ZrO_2$	$7NiCuZrO_2$	$8NiCu/ZrO_2$	$10NiCu/ZrO_2$
2-MF yield (%)	3.6	6.9	3.5	1.3	2.4
FA yield (%)	62.8	86.5	93.0	81.0	37.2
Other (%)	5.9	3.5	2.7	2.6	2.1
FF conv. (%)	75.2	97.9	99.5	88.8	65.3

Reaction condition; catalyst: 0.2 g, FF: 0.5 g, IPA: 23 g, n-decane: 0.016 g, 200 °C, 4 h., 1.5 MPa H_2.

65.3% FF conversion for 0.1 g Ni amount in the catalyst. From XPS analysis, the surface ratio of the Cu/Ni in the catalysts was calculated and it was observed that the surface ratio of the Cu/Ni decreased from 1.09 to 0.91 with the increasing of Ni amount from 0.07 g to 0.1 g in the catalyst. Liu *et al.,*[42] also showed the increasing Ni amount effect in their reactions and they concluded that due to the higher Ni amount, particle accumulation may affect the catalyst activity negatively.

The effect of Cu amount in the catalyst on the FF hydrogenation was also researched using the most effective Ni-Cu/ZrO_2 catalyst with 0.07 g Ni.

Ni-Cu/ZrO_2 catalysts containing Cu in amounts ranging from 0.05 g to 0.15 g at a fixed ratio of 7% Ni were prepared to study the effect of Cu amount on the reactions. The reactions were performed using these catalysts at 200 °C for 4 h under 1.5 MPa H_2 pressure at ambient temperature, and FA, MF yields and FF conversions are given in Table 5. Cu is also effective on FF hydrogenation to FA. FA yield and FF conversion increased and by-product (other) decreased with the increase in the amount of Cu from 0.05 g to 0.1 g in the Ni-Cu/ZrO_2 catalyst. However, the maximum 5.7% 2-MF yield was obtained with the catalyst containing 0.05 g Cu and 2-MF yield slightly decreased with the increase in Cu amount of the catalyst. The maximum FA yield of 93% was achieved with the catalyst containing 0.1 g Cu and then decreased to 58.0% in the presence of the catalyst with 0.15 g Cu. In the light of the studies on the amount of Ni and Cu in the catalysts, the most effective catalyst was chosen as Ni-Cu/ZrO_2 with 0.07 g Ni and 0.1 g Cu and further reactions were carried out using this catalyst.

In order to see the effects of Ni and Cu on the reactions separately, Ni/ZrO_2 with 0.07 g Ni and Cu/ZrO_2 with 0.1 g Cu were prepared and their effectiveness on the hydrogenation of FF was examined. As seen in Table 6, Compared to 7Ni/ZrO_2 catalyst, the effectiveness of Cu/ZrO_2 catalyst on FF conversion is higher. The 10Cu/ZrO_2 catalyst also gave 84.2% FA yield. However, when Ni and Cu were together in the catalyst structure, FA yield increased to 93%. The by-product (other) also decreased from 6.7% to 2.7% by using the 7Ni-Cu/ZrO_2 catalyst. In our previous study on investigating the effect of Cu amount, reaction temperature, pressure, time and catalyst loading on FF hydrogenation with the Cu/ZrO_2 sol-gel catalyst, a maximum FA yield of 79.8% could be achieved.[9]

Table 6. The effect of reduction of 7Ni/ZrO_2, 10Cu/ZrO_2 and 7Ni-Cu/ZrO_2 catalysts on FA, 2-MF yields and FF conversion.

Catalyst	7Ni/ZrO_2	10Cu/ZrO_2	7Ni-Cu/ZrO_2
2-MF yield (%)	–	8.1	3.5
FA yield (%)	9.1	84.2	93.0
Other	1.3	6.7	2.7
FF conversion (%)	12.5	99.5	99.7

Reaction condition; catalyst: 0.2 g, FF: 0.5 g, IPA: 23 g, n-decane: 0.016 g, 200 °C, 4 h., 1.5 MPa H_2.

3.2b *The effect of reaction parameters on furfural hydrogenation using Ni-Cu/ZrO_2 catalyst*: The effect of hydrogen pressure on the hydrogenation reactions was investigated under 1.0, 1.5 and 2.0 MPa H_2 at ambient temperature with 7Ni-Cu/ZrO_2 catalyst containing 0.07 g Ni and 0.1 g Cu and FF conversion and product yields are shown in Figure 11. The change of H_2 pressure from 1.0 MPa to 1.5 MPa played an important role on FF conversion and FA yield. With the increase in hydrogen pressure from 1.0 MPa to 1.5 MPa, FA yield increased from 47.1% to 93% and FA conversion reached 99.7% from 77.2%. However, the highest 93.0% FA yield decreased to 86.6% and 2-MF yield increased to

Table 5. The effect of Cu amount in Ni-Cu/ZrO_2 catalyst with 0.07 g Ni on FA, 2-MF yields and FF conversion.

Catalyst	Ni5Cu/ZrO_2	Ni7.5Cu/ZrO_2	Ni10CuZrO_2	Ni12.5Cu/ZrO_2	Ni15Cu/ZrO_2
2-MF yield (%)	5.7	4.3	3.5	3.6	3.5
FA yield (%)	50.3	81.1	93.0	90.8	58.0
Other (%)	4.7	3.7	2.7	3.0	4.5
FF conv. (%)	65.1	91.3	99.7	97.4	70.7

Reaction condition; catalyst: 0.2 g, FF: 0.5 g, IPA: 23 g, n-decane: 0.016 g, 200 °C, 4 h., 1.5 MPa H_2.

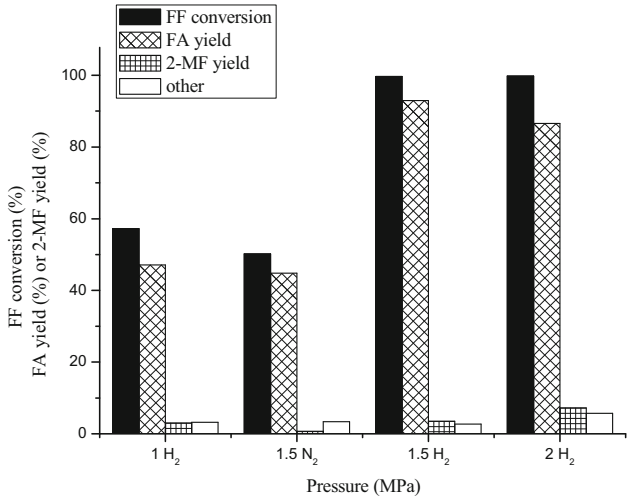

Figure 11. The effect of H_2 and N_2 pressure on FA, 2-MF yields and FF conversion using the 7Ni-Cu/ZrO_2 catalyst. Reaction condition: FF: 0.5 g, IPA: 23 g, n-decane: 0.016 g, 200 °C, 4 h.

7.2% under 2.0 MPa H_2 pressure. Higher hydrogen pressure supports the reaction towards the formation of MF from FA and by-product (other).[9,10,43] The reaction was also carried out under 1.5 MPa nitrogen pressure at same reaction conditions. However, 44.8% FA with 50.2% FF conversion could be obtained, indicating that IPA is also playing a role as a hydrogen donor.

The effect of the catalyst loading on FF hydrogenation was searched using different amounts of catalyst ranging from 0.15 g to 0.25 g. FF conversion, FA and MF yields are shown in Figure 12. FF conversion and FA yield rose when the catalyst amount increased from 0.15 g to 0.2 g in the reactions. However, FA yield decreased from 93% to 88.1% using 0.25 g catalyst and on the other hand, 2-MF yield increased to 8.1% with 0.25 g catalyst amount. It means that the increase in the catalyst amount up to 2.5 g provides the hydrogenation/hydrogenolysis reactions[9,43] and the reaction continues to form 2-MF from FA. Optimal catalyst content is 0.2 g to convert 0.5 g FF to FA at 200 °C for 4 h under 1.5 MPa H_2 pressure. 0.2 g catalyst was used for the following reactions.

The temperature is one of the most important parameters on the reactions. To examine the effect of the temperature on hydrogenation reactions of FF, reactions were realized at temperatures ranging from 160 °C to 220 °C for 4 h under 1.5 MPa H_2 pressure. The product yields and FF conversions are seen in Figure 13. FF conversion and FA yield increased gradually with a temperature rise. FA yield reached 93% with 99.7% FF conversion and then decreased to 66.2% at 220 °C. The reaction tends to the formation of 2-MF at a temperature higher than 200 °C.[9,10] However, even the temperature rise was not enough to increase 2-MF yield too much. 2-MF yield was only up to 21.9% at 220 °C. The increase in the temperature also increased the by-product (other). The most effective temperature to obtain FA is 200 °C using the 7Ni-Cu/ZrO_2 catalyst for 4 h under 1.5 MPa H_2 pressure.

The reaction time is also one of the most important parameters on the reactions. Reactions were performed for holding times ranging from 1 to 5 h at 200 °C to examine the effect of the reaction time on FF hydrogenation to FA. FF conversion, FA and 2-MF yields

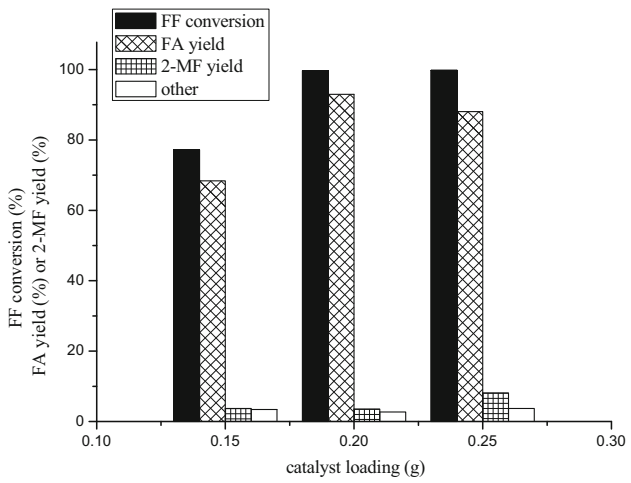

Figure 12. The effect of different catalyst amount on FA, 2-MF yields and FF conversion using the 7Ni-Cu/ZrO_2 catalyst. Reaction condition: FF: 0.5 g, IPA: 23 g, n-decane: 0.016 g, 200 °C, 4 h., 1.5 MPa H_2.

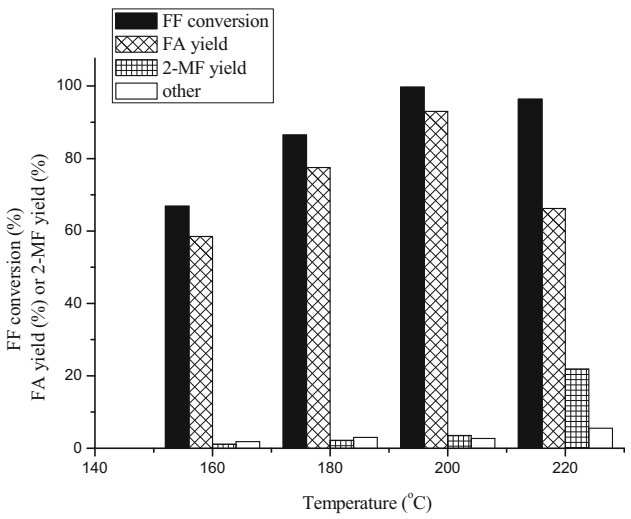

Figure 13. The effect of reaction temperature on FA, 2-MF yields and FF conversion using the 7Ni-Cu/ZrO_2 catalyst. Reaction condition: catalyst: 0.2 g, FF: 0.5 g, IPA: 23 g, n-decane: 0.016 g, 4 h., 1.5 MPa H_2.

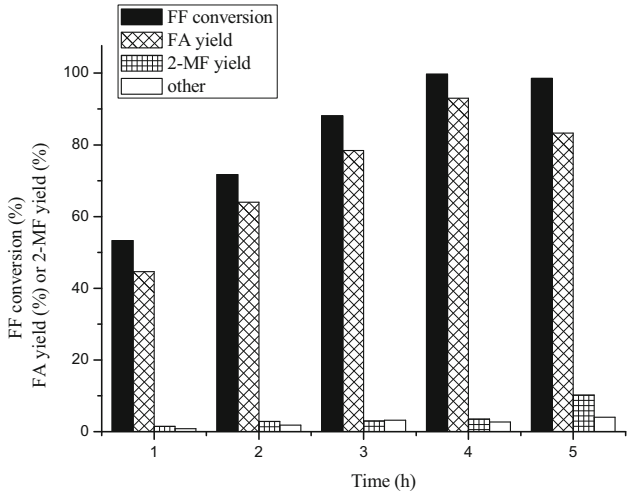

Figure 14. The effect of reaction time on FA, 2-MF yields and FF conversion using the 7Ni-Cu/ZrO_2 catalyst. Reaction condition: catalyst: 0.2 g, FF: 0.5 g, IPA: 23 g, n-decane: 0.016 g, 200 °C, 1.5 MPa H_2.

are exhibited in Figure 14. Both FF conversion and FA yield increased significantly with increasing reaction time. FA yield reached 93% in the fourth hour. However, FA yield decreased from 93% to 83.3% and 2-MF yield increased to 10.2% after 5 h. After 4 h, hydrogenation reaction of FF proceeded to form 2-MF from FA.[9] The increase of the reaction time also caused to raise the amount of the by-product (other).

The 7Ni-Cu/ZrO_2 catalyst was also reduced at 500 °C under 10% H_2/N_2 gas mixture for 1 h and the effect of the reduction on the reaction at the temperatures of 180 °C and 200 °C under 1.5 MPa H_2 pressure and at the temperature of 200 °C under 1 MPa H_2 pressure was investigated. As seen in Table 7, at the same reaction conditions, the unreduced catalyst is more active than the reduced catalyst for FF hydrogenation. Both FF conversion and FA yield is higher with unreduced catalyst.

Different Cu-Ni catalysts were tested by researchers in the literature. Liu *et al.,*[42] studied on bimetallic Cu-Ni/CNTs catalysts for the hydrogenation of FF, however, their bimetallic Cu-Ni catalysts showed 100% conversion of FF and up to 90.3% selectivity towards THFA at 130 °C, 40 bar hydrogen and 10 h reaction time. Khromova *et al.,*[16] investigated FF hydrogenation using the reduced sol-gel Ni-Cu catalyst on SiO_2 at 250 and 300 °C. They achieved 100% FA selectivity with approximately 80% FF conversion using the reduced catalyst at 250 °C at 110 °C under 6 MPa pressure. However, they concluded that higher reduction temperature favors further FA hydrogenation to THFA due to nickel oxide reduction to the metallic Ni. On the other hand, Srivastava *et al.,*[12] reported 2-MF selectivity of 81.6% with 100% FF conversion at 200 °C and 93.6% FA selectivity at 92.6% FF conversion at 130 °C under 4 MPa after 4 h with Cu-Ni/Al_2O_3 catalyst in their study. Zhang *et al.,*[44] also synthesized the Cu-Ni/Al_2O_3 catalyst for FF hydrogenation and obtained 82.5% 2-MF+2MTHF yields with 100% FF conversion at 230 °C for 4 h in isopropanol. Seemala *et al.,*[15] investigated the effects of Cu−Ni bimetallic catalyst composition and support (Al_2O_3 and TiO_2) on FF hydrogenation at 200 °C under 35 bar H_2. In their results, FF is converted to primarily 2-MF when TiO_2 is used as a support, FA and THFA are the primary reaction products when the support is Al_2O_3. In our study, 93% FA yield at 99.7% FF conversion was achieved with the Ni-Cu/ZrO_2 catalyst at 200 °C for 4 h under 1.5 MPa H_2 initial pressure which is lower than the pressure used in other studies.

The reaction results on FF hydrogenation with Ni-Cu/ZrO_2 catalysts exhibited that the main reaction product was FA. The sol-gel Ni-Cu/ZrO_2 catalyst without the use of expensive noble metals is comparatively active on FF hydrogenation to FA in mildly hydrogen pressure. From our previous studies, it is

Table 7. The effect of the reduced catalyst on the reactions.

Reaction condition	180 °C-1.5 MPa	180 °C-1.5 MPa[a]	200 °C 1.5 MPa	200 °C-1.5 MPa[a]	200 °C-1 MPa	200 °C-1 MPa[a]
2-MF yield (%)	2.2	1.8	3.5	4.1	3	1.9
FA yield (%)	77.5	71.2	93	79.4	47.1	27.3
Other (%)	3	2.7	2.7	3.6	3.2	3.6
FF conv. (%)	86.5	78.9	99.7	90.1	57.2	34.1

[a]Reduced catalyst was used.

known that the Cu/ZrO_2 sol-gel catalyst promotes FA formation.[9,10] The addition of Ni to Cu/ZrO_2 catalyst increased the catalytic activity due to the synergistic effect of nickel and copper structures in the ZrO_2. Co structure in $Co\text{-}Cu/ZrO_2$ catalyst also positively affected the reactions.[10] However, Co structure was effective on 2-MF synthesis, Ni structure supports the reactions on FA formation. As resulted in TPR analysis, it is revealed that Cu^{2+} is reduced at 200 °C and Ni^{2+} is reduced at around 500 °C. Therefore, it is understood that Cu^{2+} was reduced and Ni^{2+} remains unreduced in the reaction condition. From XPS results it is also understood that Cu^{2+} was reduced to Cu^0/Cu^+ by the adsorbed hydrogen on the catalyst surface. Ni^{2+} was not reduced to metallic Ni during hydrogenation reactions. XRD pattern of 1st used and 5th used catalysts also showed the formation of Cu^o. It can be suggested that Cu^0/Cu^+ sites on catalyst surface provide the adsorption of the carbonyl group of FF on Cu^0/Cu^+ which promotes the hydrogenation of the carbonyl group.[9,10,42,45] Moreover, the presence of Ni^{2+} sites on the catalyst surface may provide the synergistic hydrogen spillover effect on FF hydrogenation to FA.

The reactions were carried out for five times with the same $7Ni\text{-}Cu/ZrO_2$ catalyst at 200 °C for 4 h under 1.5 MPa H_2 pressure to test the reusability of the catalyst. The catalyst was removed from the reaction solution and calcined at 500 °C for 30 min to reactivate the catalyst after each reaction was completed. FF conversion, FA and 2-MF yields are shown in Figure 15. FF conversion decreased from 99.7% to 82.4% and FA yield also decreased from 93% to 77.4% in the 2nd use. The used catalyst was also tested without calcination. The filtrated catalyst was washed three times in IPA and dried. However, when the used catalyst without calcination was used in the second time, FF conversion and FA yield decreased to 52.7% and 39.2%, respectively, indicating that the carbonaceous species accumulate on the catalyst surface. In subsequent uses, the calcination was applied to the catalyst and the rate of decrease in FA yield decreased and FA yield was 70.8% with 74.6% FF conversion in the 5th use. The BET surface area of fresh $7Ni\text{-}Cu/ZrO_2$ also decreased from 45.1 to 14.5 m^2g^{1-}. The reduction of surface area may be attributed to further crystallization due to the calcination and sintering. The reduction in the efficiency of the catalyst may be due to the decrease in the surface area of the catalyst.[9,10,46]

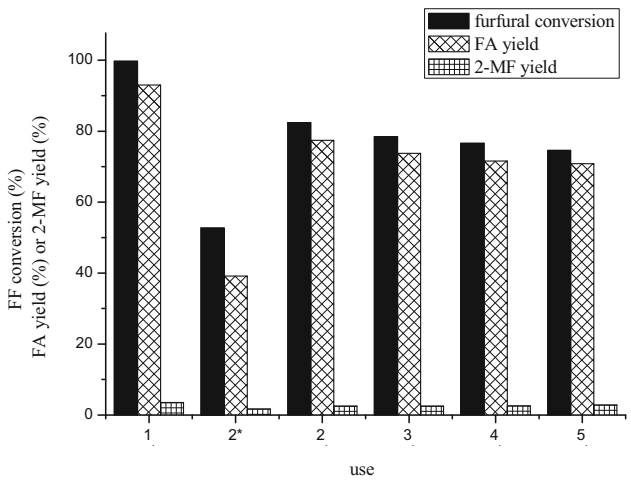

Figure 15. Reusability of the $7Ni\text{-}Cu/ZrO_2$ catalyst. Reaction condition: catalyst: 0.2 g, FF: 0.5 g, IPA: 23 g, n-decane: 0.016 g, 200 °C, 4 h., 1.5 MPa H_2, 2*: catalyst used without calcination.

4. Conclusions

$Ni\text{-}Cu/ZrO_2$ sol-gel catalyst was synthesized and investigated for the hydrogenation of FF reactions. To understand the effect of Ni and Cu loading amount in the catalyst, $Ni\text{-}Cu/ZrO_2$ catalysts were synthesized with different ratios of Cu and Ni. Cu/ZrO_2 and Ni/ZrO_2 catalysts were also prepared to compare the effect of the $Ni\text{-}Cu/ZrO_2$ catalyst. The reaction results exhibited the synergistic effect of Ni and Cu in the catalyst structure and both Ni and Cu were effective on FA formation. The reactions were detailed by using the $7Ni\text{-}Cu/ZrO_2$ catalyst under different reaction conditions. The $Ni\text{-}Cu/ZrO_2$ catalyst gave 93% FA yield at 200 °C for 4 h under 1.5 MPa H_2 initial pressure. The increase in the temperature, time, hydrogen pressure and catalyst loading promoted the reaction forward to 2-MF formation, slightly. The sol-gel $Ni\text{-}Cu/ZrO_2$ catalyst without reduction showed comparatively good activity on the hydrogenation of FF to FA at mild reaction pressure.

Acknowledgements

This study was funded by the Scientific Research Projects Coordination Unit of Istanbul University-Cerrahpasa. Project Number: FYL-2020-34532.

Conflict of interest There is no conflict of interest to declare.

References

1. Werpy T, Petersen G, Aden A, Bozell J J, Holladay J, White J, Manheim A, Elliot D, Lasure L, Jones S, Gerber M, Ibsen K, Lumberg L and Kelly S 2004 US Department of Energy, report NREL/TP-510-355532

2. Mariscal R, Maireles-Torres P, Ojeda M, Sádaba I and Granados M L 2016 Furfural: a renewable and versatile platform molecule for the synthesis of chemicals and fuels *Energy Environ. Sci*. **9** 1144
3. Nagaraja B M, Padmasri A H, Raju B D and Rama R K S 2007 Vapor phase selective hydrogenation of furfural to furfuryl alcohol over Cu–MgO coprecipitated catalysts *J. Mol. Catal. A: Chem.* **265** 90
4. Yan K, Wu G, Lafleur T and Jarvis C 2014 Production, properties and catalytic hydrogenation of furfural to fuel additives and value-added chemicals *Renew. Sust. Energ. Rev.* **38** 663
5. Panagiotopoulou P and Vlachos D G 2014 Liquid phase catalytic transfer hydrogenation of furfural over a Ru/C catalyst *Appl. Catal. A-Gen.* **480** 17
6. Liu L, Lou H and Chen M 2018 Selective hydrogenation of furfural over Pt based and Pd based bimetallic catalysts supported on modified multiwalled carbon nanotubes (MWNT) *Appl. Catal. A-Gen.* **550** 1
7. Li F, Cao B, Ma R, Liang J and Song H 2016 Performance of Cu/TiO_2-SiO_2 catalysts in hydrogenation of furfural to furfuryl alcohol *Can. J. Chem. Eng.* **94** 1368
8. Chen H, Ruan H, Lu X, Fu J, Langrish T and Lu X 2018 Efficient catalytic transfer hydrogenation of furfural to furfuryl alcohol in near-critical isopropanol over Cu/MgO-Al_2O_3 catalyst *Mol. Catal.* **445** 94
9. Algorabi S, Akmaz S and Koç S N 2020 The investigation of hydrogenation behavior of furfural over sol-gel prepared Cu/ZrO_2 catalysts *J. Sol-Gel Sci. Technol.* **96** 47
10. Akmaz S, Algorabi S and Koç S N 2020 Furfural hydrogenation to 2-methylfuran over efficient sol-gel copper-cobalt/zirconia catalyst *Can. J. Chem. Eng.*
11. Fulajtarova K, Sotak T, Hronec M, Vavra I and Dobrocka E 2015 Aqueous phase hydrogenation of furfural to furfuryl alcohol over Pd–Cu catalysts *Appl. Catal. A-Gen.* **502** 78
12. Srivastava S, Jadeja G C and Parikh J 2018 Copper-cobalt catalyzed liquid phase hydrogenation of furfural to 2-methylfuran: An optimization, kinetics and reaction mechanism study *Chem. Eng. Res. Des.* **132** 313
13. Fu Z, Wang Z, Lin W, Song W and Li S 2017 High efficient conversion of furfural to 2-methylfuran over Ni-Cu/Al_2O_3 catalyst with formic acid as a hydrogen donor *Appl. Catal. A- Gen.* **547** 248
14. Sulmonetti T P, Pang S H, Claure M T, Lee S., Cullen D A, Agrawal P K and Jones C W 2016 Vapor phase hydrogenation of furfural over nickel mixed metal oxide catalysts derived from layered double hydroxides *Appl. Catal. A-Gen*. **517** 187
15. Seemala B, Cai C M, Kumar R, Wyman C E and Christopher P 2018 Effects of Cu−Ni bimetallic catalyst composition and support on activity, selectivity, and stability for furfural conversion to 2 methyfuran *ACS Sustain. Chem. Eng.* **6** 2152
16. Khromova S A, Bykova M V, Bulavchenko O A, Ermakov D Y, Saraev A A, Kaichev V V, Venderbosch R H and Yakovlev V A 2016 Furfural hydrogenation to furfuryl alcohol over bimetallic Ni–Cu sol–gel catalyst: A model reaction for conversion of oxygenates in pyrolysis liquids *Top. Catal.* **59** 1413
17. Wu J, Gao G, Li J, Sun P, Long X and Li F 2017 Efficient and versatile CuNi alloy nanocatalysts for the highly selective hydrogenation of furfural *Appl. Catal. B- Environ.* **203** 227
18. Wang Y and Caruso R A 2002 Preparation and characterization of CuO–ZrO_2 nanopowders, *J. Mater. Chem.* **12** 1442
19. XPS Interpretation of Nickel. https://xpssimplified.com/elements/nickel.php (accessed July 2020).
20. Valente J S, Valle-Orta M, Armendáriz-Herrera H, Quintana-Solórzano R, Angel P, Ramírez-Salgado J and Montiel-López J R 2018 Controlling the redox properties of nickel in NiO/ZrO_2 catalysts synthesized by sol–gel *Catal. Sci. Technol.* **8** 4070
21. Heracleous E, Lee A F, Wilson K and Lemonidou A A 2005 Investigation of Ni-based alumina-supported catalysts for the oxidative dehydrogenation of ethane to ethylene: structural characterization and reactivity studies *J. Catal.* **231** 159
22. Solsona B, López Nieto J M, Concepción P, Dejoz F, Ivars A and Vázquez M I 2011 Oxidative dehydrogenation of ethane over Ni-W-O mixed metal oxide catalysts *J. Catal.* **280** 28
23. Carley A F, Jackson S D, Roberts M W and O'Shea J 2000 Alkali metal reactions with Ni(110)–O and NiO(100) surfaces *Surf. Sci.* **454** 141
24. Rao C N R, Vijayakrishnan V, Kulkarni G U and Rajumon M K 1995 A comparative study of the interaction of oxygen with clusters and single-crystal surfaces of nickel *Appl. Surf. Sci.* **84** 285
25. Watts J F and Wolstenholme J 2003 in *An Introduction to Surface Analysis by XPS and AES* (England: John Wiley)
26. Peck M A and Langell M A 2012 Comparison of nanoscaled and Bulk NiO Structural and Environmental Characteristics by XRD, XAFS, and XPS *Chem. Mater.* **24** 4483
27. Kim K S and Winograd N 1974 X-ray photoelectron spectroscopic studies of nickel-oxygen surfaces using oxygen and argon ion-bombardment *Surf. Sci.* **43** 625
28. Shen Y and Lua A C 2014 Sol–gel synthesis of Ni and Ni supported catalysts for hydrogen production by methane decomposition *RSC Adv.* **4** 42159
29. Bykova M V, Ermakov D Y, Kaichev V V, Bulavchenko O A, Saraev A A, Lebedev M Y and Yakovlev V A 2012 Ni-based sol–gel catalysts as promising systems for crude bio-oil upgrading:Guaiacol hydrodeoxygenation study *Appl. Catal. B-Environ*. **113–114** 296
30. Han S J, Song J H, Bang Y, Yoo J, Park S, Kang K H and Song I K 2016 Hydrogen production by steam reforming of ethanol over mesoporous Cu-Ni-Al_2O_3-ZrO_2 xerogel catalysts *Int. J. Hydrogen Energ.* **41** 2554
31. Siddiqui N, Roy A S, Goyal R, Khatun R, Pendem C, Chokkapu A N, Bordoloi A and Bal R 2018 Hydrogenation of 5 hydroxymethylfurfural to 2,5 dimethylfuran over nickel supported tungsten oxide nanostructured catalyst *Sustain. Energ. Fuels* **2** 191
32. Liu Z, Amiridis M D and Chen Y 2005 Characterization of CuO supported on tetragonal ZrO_2 catalysts for N_2O decomposition to N_2 *J. Phys. Chem. B* **109** 1251
33. Wang L C, Liu Q, Chen M, Liu Y M, Cao Y, He H Y and Fan K N 2007 Structural evolution and catalytic

properties of nanostructured Cu/ZrO_2 catalysts prepared by oxalate gel-coprecipitation technique *J. Phys. Chem. C* **111** 16549
34. Ehsan M A, Hakeem A S, Khaledi H, Mazhar M, Shahid M M, Pandikumar A and Huang N M 2015 Fabrication of CuO–1.5ZrO_2 composite thin film, from heteronuclear molecular complex and its electrocatalytic activity towards methanol oxidation *RSC Adv.* **5** 103852
35. Nguyen-Huy C, Lee H, Lee J, Kwak J H and An K 2019 An Mesoporous mixed CuCo oxides as robust catalysts for liquid-phase furfural hydrogenation *Appl. Catal. A-Gen.* **571** 118
36. Akgul F A, Akgul G, Yildirim N, Unalan H E and Turan R. 2014 Influence of thermal annealing on microstructural, morphological, optical properties and surface electronic structure of copper oxide thin films *Mater. Chem. Phys.* **147** 987
37. Biesinger M C, Lau L W M, Gerson A R and Smart R St C 2010 Resolving surface chemical states in XPS analysis of first row transition metals, oxides and hydroxides: Sc, Ti, V, Cu and Zn *Appl. Surf. Sci.* **257** 887
38. Kim J P, Pak E S, Hong T E, Bae J S, Ha M G, Jin J S, Jeong E D and Hong K S 2012 Electric properties and chemical bonding states of pn-junction p-CuO/n-Si by sol-gel method *J. Ceram. Process Res.* **13** 96
39. Jiang P, Prendergast D, Borondics F, Porsgaard S and Giovanetti L 2013 Experimental and theoretical investigation of the electronic structure of Cu_2O and CuO thin films on Cu(110) using x-ray photoelectron and absorption spectroscopy *J. Chem. Phys.* **138** 024704-1-6
40. Ling P, Zhang Q, Cao T and Gao F 2018 Versatile three-dimensional porous Cu@Cu_2O aerogel networks as electrocatalysts and mimicking peroxidases *Angew. Chem. Int. Ed.* **57** 6819
41. Liu J, Liao M, Imura M, Tanaka A, Iwai H and Koide Y 2014 Low on-resistance diamond field effect transistor with high-k ZrO_2 as dielectric *Sci. Rep.* **4** 6395
42. Liu L, Lou H and Chen M 2016 Selective hydrogenation of furfural to tetrahydrofurfuryl alcohol over Ni/CNTs and bimetallic Cu-Ni/CNTs catalysts *Int. J. Hydrogen Energ.* **41** 14721
43. Wang Y, Miao Y, Li S, Gao L and Xiao G 2017 Metal-organic frameworks derived bimetallic Cu-Co catalyst for efficient and selective hydrogenation of biomass-derived furfural to furfuryl alcohol *Mol. Catal.* **436** 128
44. Zhang Z, Pei Z, Chen H, Chen K, Hou Z, Lu X, Ouyang P and Fu J 2018 Catalytic in-situ hydrogenation of furfural over bimetallic Cu−Ni alloy catalysts in isopropanol *Ind. Eng. Chem. Res.* **57** 4225
45. Srivastava S, Jadeja G C and Parikh J 2017 Synergism studies on alumina-supported copper-nickel catalysts towards furfural and 5-hydroxymethylfurfural hydrogenation *J. Mol. Catal. A: Chem.* **426** 244
46. Zhang J and Chen J 2017 Selective transfer hydrogenation of biomass-based furfural and 5-hydroxymethylfurfural over hydrotalcite-derived copper catalysts using methanol as a hydrogen donor *ACS Sustain. Chem. Eng.* **5** 5982